On Uplink Asynchronous Non-Orthogonal Multiple Access Systems with Timing Error

Xun Zou, Biao He, and Hamid Jafarkhani
Center for Pervasive Communications and Computing, University of California, Irvine, CA, 92697
Email: {xzou4, biao.he, hamidj}@uci.edu

***Abstract*—Recent studies have shown that asynchronous non-orthogonal multiple access (ANOMA) outperforms conventional synchronous non-orthogonal multiple access (NOMA) by taking advantage of artificial timing mismatch with oversampling. For the first time, we comprehensively study the impact of timing errors on the performance of uplink ANOMA systems in this paper. We consider two types of timing errors, which are the synchronization timing error and the coordination timing error. We analyze how the timing errors affect ANOMA systems, and derive the throughput loss of ANOMA systems incurred by both the synchronization timing error and the coordination timing error. An interesting finding is that the synchronization timing error has a larger impact on the throughput performance of ANOMA systems compared with the coordination timing error.**

I. Introduction

Non-orthogonal multiple access (NOMA) is envisaged as a promising technique for future radio access [1]. Traditional orthogonal multiple access (OMA) techniques allocate orthogonal resources to different users, e.g., orthogonal time resources in time division multiple access (TDMA). Differently, the NOMA provides the multiuser access by allocating non-orthogonal resources to users [2].

Another line of research is to study the effects of symbol-asynchrony on the performance of the wireless communication systems, from Verdu's pioneer work in [3] to the very recent studies, e.g., [4–8]. In particular, adding intentional delays to improve the performance has been considered in, e.g., [9] and references therein.

Recently, a transmission scheme combining the NOMA and the symbol-asynchronous transmission, namely asynchronous NOMA (ANOMA) has been proposed in [10]. The ANOMA intentionally creates symbol asynchronism between users as an additional resource to address the problem of inter-user interference in NOMA systems. It has been shown that the ANOMA significantly outperforms the conventional (synchronized) NOMA by achieving a larger throughput. It is worth mentioning that a similar concept to the ANOMA in [10] was also proposed in [8].

For the ANOMA, timing information plays a vital role in the system design, and the performance of ANOMA is directly related to the accuracy of timing information. This is because the composite symbol-asynchronous signals are sampled multiple times by using multiple matched filters, which are designed according to the timing information of each signal component. Such a method is also known as the asynchronous oversampling [4, 8], which takes advantage of the sampling diversity to achieve the rate performance gain. In the existing studies on the ANOMA [8, 10], the timing information of each signal component is ideally assumed to be perfectly known. However, the timing information in practice cannot always be perfectly obtained, and the timing errors are often inevitable.

In this paper, we comprehensively study the impact of timing errors on the performance of uplink ANOMA systems. Two types of timing errors are taken into consideration, i.e., the synchronization timing error and the coordination timing error. The synchronization timing error accounts for the error caused in signal synchronization, i.e., the time that the signal is received, and the coordination timing error captures the coordination error of the timing mismatch between asynchronous signals. To the best of our knowledge, we are the first to investigate the ANOMA systems with timing errors. We derive the expressions for the throughput loss of ANOMA systems incurred by the timing errors, and analyze how the synchronization timing error and the coordination timing error individually affect the ANOMA. Our results show that the synchronization timing error deteriorates the system performance more severely than the coordination timing error. The remainder of the paper is organized as follows. The system model is presented in Section II. We analyze the outputs of ANOMA matched filters with timing errors and the average throughput loss incurred by timing errors in Sections III and IV, respectively. The numerical results are shown in Section V. Finally, we draw the conclusions in Section VI.

Notations: $(\cdot)^H$ denotes the Hermitian transpose, $(\cdot)^T$ denotes the transpose, $\mathrm{Tr}(\cdot)$ denotes the trace operation, $(\cdot)^{-1}$ denotes the inverse operation, $|x|$ denotes the absolute value of x, $\mathbb{E}[\cdot]$ denotes the expectation operation, $\mathcal{CN}(0,1)$ denotes the complex normal distribution with zero mean and unit variance, and $\mathbf{1}(\cdot)$ denotes the unit step function whose value is zero for negative argument and one for positive argument.

II. System Model

In this paper, we consider an uplink system which consists of a single BS and two users, as shown in Fig. 1. The two users share the same frequency-time resource to transmit signals to the BS. We employ the block fading model, such that the

This work was supported in part by the NSF Award CCF-1526780.

978-1-5386-3180-5/18/$31.00 ©2018 IEEE

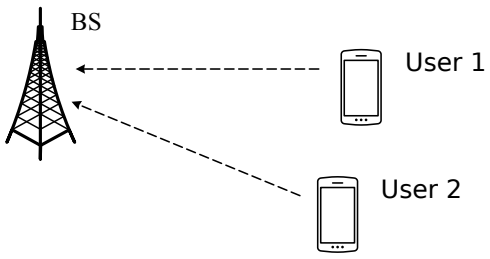

Fig. 1: Illustration of a two-user uplink system.

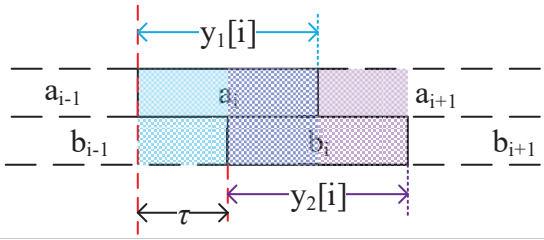

Fig. 2: Illustration of the sampling for ANOMA.

channel coefficients remain constant during the transmission of a block of symbols, and change independently from one block to the next. We assume that perfect channel state information (CSI) is known at the BS via the uplink channel training.

A. ANOMA

Different from the conventional NOMA, the ANOMA intentionally introduces a symbol-asynchronism between the message packets of different users. Denote the intended timing mismatch between the symbols of Users 1 and 2 by τ. Without loss of generality, we assume that $0 < \tau < T$, where T denotes the duration of each symbol.

Let $a_i = h_1\sqrt{P_1}s_1[i]$ and $b_i = h_2\sqrt{P_2}s_2[i]$, where the subscripts 1 and 2 denote the parameters for Users 1 and 2, respectively, $s[i]$ denotes the ith normalized transmitted symbol, h denotes the channel coefficient, and P denotes the transmit power. The received signal at the BS is then given by

$$y(t) = \sum_{i=0}^{N-1} a_i p(t - iT) + b_i p(t - iT - \tau) + n(t), \quad (1)$$

where N denotes the total number of transmitted symbols, $p(\cdot)$ denotes the pulse-shaping filter with non-zero duration of T, and $n(t) \sim \mathcal{CN}(0, 1)$ denotes the normalized AWGN. Without loss of generality, we assume that the rectangular pulse shape is adopted, i.e., $p(t) = 1/T$ when $t \in [0, T]$ and $p(t) = 0$ when $t \notin [0, T]$.

The oversampling technique is adopted at the BS to take advantage of sampling diversity in the asynchronous systems [4]. As shown in Fig. 2, the BS uses two matched filters to obtain two sample vectors, denoted by $[y_1[1], \cdots, y_1[N]]^T$ and $[y_2[1], \cdots, y_2[N]]^T$. Specifically, the ith element in the first sample vector is given by

$$\begin{aligned} y_1[i] &= \int_{(i-1)T}^{iT} y(t)p(t - iT)dt \\ &= \int_{(i-1)T}^{iT} [a_i p(t - iT) + b_{i-1}p(t - (i-1)T) \\ &\quad + b_i p(t - iT)]\, p(t - iT)dt + n_1[i] \\ &= a_i + \tau b_{i-1} + (1 - \tau)b_i + n_1[i], \end{aligned} \quad (2)$$

where $n_1[i] = \int_{(i-1)T}^{iT} n(t)p(t-iT)dt$ denotes the additive noise in the sampled vector. The ith element in the second sample vector is given by

$$\begin{aligned} y_2[i] &= \int_{(i-1)T+\tau}^{iT+\tau} y(t)p(t - iT - \tau)dt \\ &= b_i + \tau a_{i+1} + (1 - \tau)a_i + n_2[i], \end{aligned} \quad (3)$$

where $n_2[i] = \int_{(i-1)T+\tau}^{iT+\tau} n(t)p(t-iT-\tau)dt$ denotes the additive noise in the sampled vector.

We can write the outputs of the two matched filters at the BS in the matrix form as

$$\mathbf{Y} = \mathbf{RHX} + \mathbf{N}, \quad (4)$$

where

$$\mathbf{Y} = [y_1[1]\ y_2[1]\ y_1[2]\ y_2[2]\ \cdots\ y_1[N]\ y_2[N]]^T, \quad (5)$$

$$\mathbf{X} = [s_1[1]\ s_2[1]\ s_1[2]\ s_2[2]\ \cdots\ s_1[N]\ s_2[N]]^T, \quad (6)$$

$$\mathbf{N} = [n_1[1]\ n_2[1]\ n_1[2]\ n_2[2]\ \cdots\ n_1[N]\ n_2[N]]^T, \quad (7)$$

$$\mathbf{R} = \begin{bmatrix} 1 & 1-\tau & 0 & \cdots & \cdots & 0 \\ 1-\tau & 1 & \tau & 0 & \cdots & 0 \\ 0 & \tau & 1 & 1-\tau & \cdots & 0 \\ \vdots & \ddots & \ddots & \ddots & \ddots & \vdots \\ 0 & \cdots & 0 & \tau & 1 & 1-\tau \\ 0 & \cdots & \cdots & 0 & 1-\tau & 1 \end{bmatrix}, \quad (8)$$

and

$$\mathbf{H} = \begin{bmatrix} h_1\sqrt{P_1} & & & & \\ & h_2\sqrt{P_2} & & & \\ & & \ddots & & \\ & & & h_1\sqrt{P_1} & \\ & & & & h_2\sqrt{P_2} \end{bmatrix}. \quad (9)$$

We assume that the transmitted symbols are independent, such that $\mathbb{E}\left[\mathbf{XX}^H\right] = \mathbf{I}$. Besides, note that the noise terms in (4) are colored due to the oversampling, and we have

$$\begin{aligned} \mathbb{E}\left\{n_1[i]n_2^H[i]\right\} &= \int_{(i-1)T}^{iT}\int_{(i-1)T+\tau}^{iT+\tau} \mathbb{E}\left\{n(t)n^H(s)\right\} \\ &\quad (t - iT)\,(s - iT - \tau)\,dtds \\ &= 1 - \tau. \end{aligned} \quad (10)$$

Thus, the covariance matrix of $\mathbf{N}$ is given by

$$\mathbf{R}_N = \mathbb{E}\left\{\mathbf{NN}^H\right\} = \mathbf{R}. \quad (11)$$

B. Timing Error

The expression for the output of the matched filters given in (4) is based on the assumption that the BS perfectly knows the timing information. However, the timing information cannot always be perfectly obtained in practice, and the timing errors are often inevitable. In this paper, we consider two types of timing errors for the ANOMA system, the synchronization timing error and the coordination timing error.

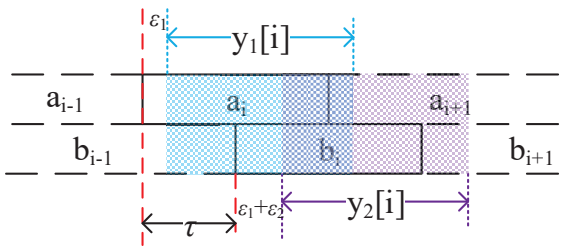

Fig. 3: Illustration of the sampling for ANOMA with timing error.

1) Synchronization Timing Error: We consider the signal from User 1 as the timing reference (the timing offset is 0), which needs the timing synchronization to the symbol from User 1 at the BS. The synchronization timing error, denoted by ϵ_1, is due to the imperfect timing synchronization. Without loss of generality, we assume that $\epsilon_1 \in (\tau - T, \tau)$. With the synchronization timing error, $y_1[i]$ is taken from the time of $(i-1)T + \epsilon_1$ to $iT + \epsilon_1$ and $y_2[i]$ is taken from the time of $(i-1)T + \tau + \epsilon_1$ to $iT + \tau + \epsilon_1$, although the BS intends to take $y_1[i]$ from the time of $(i-1)T$ to iT and $y_2[i]$ from the time of $(i-1)T + \tau$ to $iT + \tau$.

2) Coordination Timing Error: In order to achieve the desired timing mismatch between the two signals, the BS coordinates between two users to add the intended timing offsets at each transmitter. The coordination timing error, denoted by ϵ_2, results from the imperfect coordination of the timing mismatch between the users. With the coordination timing error, the actual timing mismatch becomes $\tau + \epsilon_2$, while the intended timing mismatch is τ. In addition to the synchronization timing error ϵ_1, $y_2[i]$ is taken from $(i-1)T + \tau + \epsilon_1 + \epsilon_2$ to $iT + \tau + \epsilon_1 + \epsilon_2$, although the BS intends to take $y_2[i]$ from $(i-1)T + \tau$ to $iT + \tau$. Without loss of generality, we assume that $\epsilon_1 + \epsilon_2 \in (-\tau, T - \tau)$.

Fig. 3 illustrates the sampling for an ANOMA system with timing error. It is worth mentioning that Fig. 3 presents the case when $\epsilon_1 > 0$ and $\epsilon_1 + \epsilon_2 > 0$, while our analysis is universal.

III. Outputs of ANOMA Matched Filters with Timing Error

In this section, we derive the outputs of the matched filters at the BS with both the synchronization timing error and the coordination timing error.

In the presence of timing error, the ith element of the first sample vector is given by

$$\begin{aligned}\hat{y}_1[i] = &\int_{(i-1)T+\epsilon_1}^{iT+\epsilon_1} a_i p(t - iT) p(t - iT - \epsilon_1) dt \\ &+ \mathbf{1}(-\epsilon_1) \int_{(i-1)T+\epsilon_1}^{iT+\epsilon_1} a_{i-1} p(t-(i-1)T) p(t-iT-\epsilon_1) dt \\ &+ \mathbf{1}(\epsilon_1) \int_{(i-1)T+\epsilon_1}^{iT+\epsilon_1} a_{i+1} p(t - (i+1)T) p(t - iT - \epsilon_1) dt \\ &+ \int_{(i-1)T+\epsilon_1}^{iT+\epsilon_1} b_{i-1} p(t - \tau - (i-1)T) p(i - iT - \epsilon_1) dt \\ &+ \int_{(i-1)T+\epsilon_1}^{iT+\epsilon_1} b_i p(t - \tau - iT) p(i - iT - \epsilon_1) dt \\ &+ \int_{(i-1)T+\epsilon_1}^{iT+\epsilon_1} n(t) p(i - iT - \epsilon_1) dt \\ &= a_i(1 - |\epsilon_1|) + a_{i-1}\mathbf{1}(-\epsilon_1)(-\epsilon_1) + a_{i+1}\mathbf{1}(\epsilon_1)\epsilon_1 \\ &+ b_{i-1}(\tau - \epsilon_1) + b_i(1 - \tau + \epsilon_1) + \hat{n}_1[i], \end{aligned} \tag{12}$$

and the ith element of the second sample vector is given by

$$\begin{aligned}\hat{y}_2[i] = &\int_{(i-1)T+\tau+\epsilon_1+\epsilon_2}^{iT+\tau+\epsilon_1+\epsilon_2} y(t) p(t - iT - \tau - \epsilon_1 - \epsilon_2) dt \\ &+ \int_{(i-1)T+\epsilon_1+\epsilon_2}^{iT+\epsilon_1+\epsilon_2} n(t) p(i - iT - \epsilon_1 - \epsilon_2) dt \\ &= b_i(1 - |\epsilon_1 + \epsilon_2|) + b_{i-1}\mathbf{1}(-\epsilon_1 - \epsilon_2)(-\epsilon_1 - \epsilon_2) \\ &+ b_{i+1}\mathbf{1}(\epsilon_1 + \epsilon_2)(\epsilon_1 + \epsilon_2) + a_i(\tau - \epsilon_1 - \epsilon_2) \\ &+ a_{i+1}(1 - \tau + \epsilon_1 + \epsilon_2) + \hat{n}_2[i]. \end{aligned} \tag{13}$$

We note from (12) and (13) that the first sample vector is affected by the synchronization timing error ϵ_1 only, while the second sample vector is affected by the sum of the synchronization timing error ϵ_1 and the coordination timing error ϵ_2.

With (12) and (13), we obtain the outputs of the two matched filters at the BS subject to the timing error in the matrix form as

$$\hat{\mathbf{Y}} = \hat{\mathbf{R}}\mathbf{H}\mathbf{X} + \hat{\mathbf{N}}, \tag{15}$$

where $\hat{\mathbf{Y}} = [\hat{y}_1[1]\ \hat{y}_2[1]\ \hat{y}_1[2]\ \hat{y}_2[2]\ \cdots\ \hat{y}_1[N]\ \hat{y}_2[N]]^T$, $\hat{\mathbf{N}} = [\hat{n}_1[1]\ \hat{n}_2[1]\ \hat{n}_1[2]\ \hat{n}_2[2]\ \cdots\ \hat{n}_1[N]\ \hat{n}_2[N]]^T$, and $\hat{\mathbf{R}}$ is given in (14) shown at the top of the next page. We note from (14) that some of the entries in $\mathbf{E}_1$ are nonlinear functions of ϵ_1 or $\epsilon_1 + \epsilon_2$, e.g., the absolute value of ϵ_1 and the unit step function of $\epsilon_1 + \epsilon_2$. Therefore, the expression of $\mathbf{E}_1$ relies on the signs of ϵ_1 and $\epsilon_1 + \epsilon_2$. For the sake of brevity, we present the analytical results for the case of $\epsilon_1 > 0$ and $\epsilon_1 + \epsilon_2 > 0$ in the rest of the paper, while our analytical method and findings are applicable to all the cases. In addition, we will present the numerical results in Section V for all possible cases of ϵ_1 and $\epsilon_1 + \epsilon_2$. With $\epsilon_1 > 0$ and $\epsilon_1 + \epsilon_2 > 0$, the expression of $\mathbf{E}_1$ is rewritten as

$$\begin{aligned}\mathbf{E}_1 = \epsilon_1 \underbrace{\begin{bmatrix} -1 & 1 & 1 & 0 & \cdots & \cdots & 0 \\ -1 & -1 & 1 & 1 & 0 & \cdots & 0 \\ 0 & -1 & -1 & 1 & 1 & \cdots & 0 \\ \vdots & \ddots & \ddots & \ddots & \ddots & \ddots & \vdots \\ 0 & \cdots & 0 & -1 & -1 & 1 & 1 \\ 0 & \cdots & 0 & 0 & -1 & -1 & 1 \\ 0 & \cdots & \cdots & 0 & 0 & -1 & -1 \end{bmatrix}}_{\mathbf{Z}_1} \\ + \epsilon_2 \underbrace{\begin{bmatrix} 0 & 0 & 0 & 0 & \cdots & \cdots & 0 \\ -1 & -1 & 1 & 1 & 0 & \cdots & 0 \\ 0 & 0 & 0 & 0 & 0 & \cdots & 0 \\ \vdots & \ddots & \ddots & \ddots & \ddots & \ddots & \vdots \\ 0 & \cdots & 0 & -1 & -1 & 1 & 1 \\ 0 & \cdots & 0 & 0 & 0 & 0 & 0 \\ 0 & \cdots & \cdots & 0 & 0 & -1 & -1 \end{bmatrix}}_{\mathbf{Z}_2}. \end{aligned} \tag{16}$$

The covariance matrix of $\hat{\mathbf{N}}$ is given by

$$\hat{\mathbf{R}}_N = \mathbb{E}\left\{\hat{\mathbf{N}}\hat{\mathbf{N}}^H\right\}$$

$$\hat{\mathbf{R}} = \begin{bmatrix} 1-|\epsilon_1| & 1-\tau+\epsilon_1 & \mathbf{1}(\epsilon_1)\epsilon_1 & 0 & \cdots & \cdots & 0 \\ 1-\tau-\epsilon_1-\epsilon_2 & 1-|\epsilon_1+\epsilon_2| & \tau+\epsilon_1+\epsilon_2 & \mathbf{1}(\epsilon_1+\epsilon_2)(\epsilon_1+\epsilon_2) & 0 & \cdots & 0 \\ \mathbf{1}(-\epsilon_1)(-\epsilon_1) & \tau-\epsilon_1 & 1-|\epsilon_1| & 1-\tau+\epsilon_1 & \mathbf{1}(\epsilon_1)\epsilon_1 & \cdots & 0 \\ \vdots & \ddots & \ddots & \ddots & \ddots & \ddots & \vdots \\ 0 & \cdots & \mathbf{1}(-\epsilon_1-\epsilon_2)(-\epsilon_1-\epsilon_2) & 1-\tau-\epsilon_1-\epsilon_2 & 1-|\epsilon_1+\epsilon_2| & \tau+\epsilon_1+\epsilon_2 & \mathbf{1}(\epsilon_1+\epsilon_2)(\epsilon_1+\epsilon_2) \\ 0 & \cdots & 0 & \mathbf{1}(-\epsilon_1)(-\epsilon_1) & \tau-\epsilon_1 & 1-|\epsilon_1| & 1-\tau+\epsilon_1 \\ 0 & \cdots & \cdots & 0 & \mathbf{1}(-\epsilon_1-\epsilon_2)(-\epsilon_1-\epsilon_2) & 1-\tau-\epsilon_1-\epsilon_2 & 1-|\epsilon_1+\epsilon_2| \end{bmatrix}$$

$$= \mathbf{R} + \underbrace{\begin{bmatrix} -|\epsilon_1| & \epsilon_1 & \mathbf{1}(\epsilon_1)\epsilon_1 & 0 & \cdots & \cdots & 0 \\ -\epsilon_1-\epsilon_2 & -|\epsilon_1+\epsilon_2| & \epsilon_1+\epsilon_2 & \mathbf{1}(\epsilon_1+\epsilon_2)(\epsilon_1+\epsilon_2) & 0 & \cdots & 0 \\ \mathbf{1}(-\epsilon_1)(-\epsilon_1) & -\epsilon_1 & -|\epsilon_1| & \epsilon_1 & \mathbf{1}(\epsilon_1)\epsilon_1 & \cdots & 0 \\ \vdots & \ddots & \ddots & \ddots & \ddots & \ddots & \vdots \\ 0 & \cdots & \mathbf{1}(-\epsilon_1-\epsilon_2)(-\epsilon_1-\epsilon_2) & -\epsilon_1-\epsilon_2 & -|\epsilon_1+\epsilon_2| & \epsilon_1+\epsilon_2 & \mathbf{1}(\epsilon_1+\epsilon_2)(\epsilon_1+\epsilon_2) \\ 0 & \cdots & 0 & \mathbf{1}(-\epsilon_1)(-\epsilon_1) & -\epsilon_1 & -|\epsilon_1| & \epsilon_1 \\ 0 & \cdots & \cdots & 0 & \mathbf{1}(-\epsilon_1-\epsilon_2)(-\epsilon_1-\epsilon_2) & -\epsilon_1-\epsilon_2 & -|\epsilon_1+\epsilon_2| \end{bmatrix}}_{\mathbf{E}_1}. \quad (14)$$

$$= \begin{bmatrix} 1 & 1-\tau-\epsilon_2 & 0 & \cdots & \cdots & 0 \\ 1-\tau-\epsilon_2 & 1 & \tau+\epsilon_2 & 0 & \cdots & 0 \\ 0 & \tau+\epsilon_2 & 1 & 1-\tau-\epsilon_2 & \cdots & 0 \\ \vdots & \ddots & \ddots & \ddots & \ddots & \vdots \\ 0 & \cdots & 0 & \tau+\epsilon_2 & 1 & 1-\tau-\epsilon_2 \\ 0 & \cdots & \cdots & 0 & 1-\tau-\epsilon_2 & 1 \end{bmatrix}$$

$$= \mathbf{R} + \underbrace{\begin{bmatrix} 0 & -\epsilon_2 & 0 & \cdots & \cdots & 0 \\ -\epsilon_2 & 0 & \epsilon_2 & 0 & \cdots & 0 \\ 0 & \epsilon_2 & 0 & -\epsilon_2 & \cdots & 0 \\ \vdots & \ddots & \ddots & \ddots & \ddots & \vdots \\ 0 & \cdots & 0 & \epsilon_2 & 0 & -\epsilon_2 \\ 0 & \cdots & \cdots & 0 & -\epsilon_2 & 0 \end{bmatrix}}_{\mathbf{E}_2}, \quad (17)$$

where $\mathbf{E}_2$ can be rewritten as

$$\mathbf{E}_2 = \epsilon_2 \underbrace{\begin{bmatrix} 0 & -1 & 0 & \cdots & \cdots & 0 \\ -1 & 0 & 1 & 0 & \cdots & 0 \\ 0 & 1 & 0 & -1 & \cdots & 0 \\ \vdots & \ddots & \ddots & \ddots & \ddots & \vdots \\ 0 & \cdots & 0 & 1 & 0 & -1 \\ 0 & \cdots & \cdots & 0 & -1 & 0 \end{bmatrix}}_{\mathbf{Z}_3}. \quad (18)$$

We note from (18) that the covariance matrix of noise terms is affected by the coordination timing error ϵ_2, while it is not related to the synchronization timing error ϵ_1.

IV. Impact of Timing Error on ANOMA Performance

In this section, we analyze the impact of timing errors on the performance of ANOMA systems in terms of the average throughput.

According to (15), the average throughput of the ANOMA system with timing errors is given as

$$\begin{aligned} R_e &= \frac{1}{N}\mathbb{E}\left\{\log\det\left(\mathbf{I}_{2N} + \hat{\mathbf{R}}_N^{-1}\hat{\mathbf{R}}\mathbf{H}\mathbf{H}^H\hat{\mathbf{R}}^{\mathbf{H}}\right)\right\} \\ &= \frac{1}{N}\mathbb{E}\left\{\log\det\left(\mathbf{I}_{2N}\right.\right. \\ &\quad \left.\left.+(\mathbf{R}+\mathbf{E}_2)^{-1}(\mathbf{R}+\mathbf{E}_1)\mathbf{H}\mathbf{H}^H(\mathbf{R}+\mathbf{E}_1^H)\right)\right\} \\ &= \frac{1}{N}\mathbb{E}\left\{\log\det\left(\mathbf{I}_{2N} + \left(\mathbf{I}_{2N} + (\mathbf{R}+\mathbf{E}_2)^{-1}(\mathbf{E}_1-\mathbf{E}_2)\right)\right.\right. \\ &\quad \left.\left.\cdot\mathbf{H}\mathbf{H}^H(\mathbf{R}+\mathbf{E}_1^H)\right)\right\} \\ &= \frac{1}{N}\mathbb{E}\left\{\log\det\left(\mathbf{I}_{2N} + \mathbf{H}\mathbf{H}^H\mathbf{R} + \mathbf{H}\mathbf{H}^H\mathbf{E}_1^H\right.\right. \\ &\quad \left.\left.+(\mathbf{R}+\mathbf{E}_2)^{-1}(\mathbf{E}_1-\mathbf{E}_2)\mathbf{H}\mathbf{H}^H(\mathbf{R}+\mathbf{E}_1^H)\right)\right\}. \end{aligned} \quad (19)$$

When there is no timing errors, i.e., $\epsilon_1 = \epsilon_2 = 0$, we have $\mathbf{E}_1 = \mathbf{E}_2 = \mathbf{0}$. Hence, substituting $\mathbf{E}_1 = \mathbf{E}_2 = \mathbf{0}$ into (19), we obtain the average throughput of the ANOMA system without timing error as

$$R = \frac{1}{N}\mathbb{E}\left\{\log\det\left(\mathbf{I}_{2N} + \mathbf{H}\mathbf{H}^H\mathbf{R}\right)\right\}. \quad (20)$$

From (19) and (20), we derive the average throughput loss incurred by the timing error as

$$\begin{aligned} \Delta &= R - R_e \\ &= -\frac{1}{N}\mathbb{E}\left\{\log\det\left[\mathbf{I}_{2N} + \left(\mathbf{I}_{2N} + \mathbf{H}\mathbf{H}^H\mathbf{R}\right)^{-1}\left(\mathbf{H}\mathbf{H}^H\mathbf{E}_1^H\right.\right.\right. \\ &\quad \left.\left.\left.+(\mathbf{R}+\mathbf{E}_2)^{-1}(\mathbf{E}_1-\mathbf{E}_2)\mathbf{H}\mathbf{H}^H(\mathbf{R}+\mathbf{E}_1^H)\right)\right]\right\}. \end{aligned} \quad (21)$$

A. Impact of Synchronization Timing Error

We first investigate the impact of synchronization timing error on the throughput loss and consider the practical scenario where the error is relatively small, such that $\epsilon_2 = 0$ and $\epsilon_1 \ll 1$.

In this case, by omitting high-order terms of ϵ_1, we obtain the throughput loss incurred by the synchronization timing error from (21) as

$$\begin{aligned} \Delta_{\epsilon_1} &= -\frac{1}{N}\mathbb{E}\left\{\log\det\left[\mathbf{I}_{2N} + \epsilon_1\left(\mathbf{I}_{2N} + \mathbf{H}\mathbf{H}^H\mathbf{R}\right)^{-1}\right.\right. \\ &\quad \left.\left.\cdot\left(\mathbf{H}\mathbf{H}^H\mathbf{Z}_1^H + \mathbf{R}^{-1}\mathbf{Z}_1\mathbf{H}\mathbf{H}^H(\mathbf{R}+\epsilon_1\mathbf{Z}_1^H)\right)\right]\right\} \\ &\overset{(a)}{\approx} -\frac{1}{N}\mathbb{E}\left\{\log\det\left[\mathbf{I}_{2N} + \epsilon_1\left(\mathbf{I}_{2N} + \mathbf{H}\mathbf{H}^H\mathbf{R}\right)^{-1}\right.\right. \\ &\quad \left.\left.\cdot\left(\mathbf{H}\mathbf{H}^H\mathbf{Z}_1^H + \mathbf{R}^{-1}\mathbf{Z}_1\mathbf{H}\mathbf{H}^H\mathbf{R}\right)\right]\right\} \\ &\overset{(b)}{\approx} -\frac{1}{N}\mathbb{E}\left\{\log\left(1+\epsilon_1\mathrm{Tr}(\mathbf{F}_1) + O(\epsilon_1^2)\right)\right\} \\ &\overset{(c)}{\approx} \epsilon_1 c_1, \end{aligned} \quad (22)$$

where $\mathbf{F}_1 = \left(\mathbf{I}_{2N}+\mathbf{H}\mathbf{H}^H\mathbf{R}\right)^{-1}\left(\mathbf{H}\mathbf{H}^H\mathbf{Z}_1^H+\mathbf{R}^{-1}\mathbf{Z}_1\mathbf{H}\mathbf{H}^H\mathbf{R}\right)$, $c_1 = -\frac{1}{N}\mathbb{E}\left[\mathrm{Tr}(\mathbf{F}_1)\right]$, (a) is approximated by using $\mathbf{R}+\epsilon_1\mathbf{Z} \approx \mathbf{R}$ as $\epsilon_1 \to 0$, (b) is derived using the special case of Jacobi's formula [13], i.e., $\det(\mathbf{I}+\epsilon\mathbf{A}) = 1+\epsilon\mathrm{Tr}(\mathbf{A})+O(\epsilon^2)$, and (c) is derived by omitting the high-order terms of ϵ_1 and applying the approximation $\log(1+x) \approx x$ when $x \to 0$. From (22),

we note that the rate loss is approximately linear to ϵ_1 when $\epsilon_2 = 0$ and $\epsilon_1 \ll 1$.

Remark 1: We claim that the throughput loss incurred by ϵ_1 is determined by the absolute value of the error when $\tau = T/2$, i.e., $\Delta_{\epsilon_1} = \Delta_{-\epsilon_1}$, if $\mathbb{E}\left[\mathbf{H}\mathbf{H}^H\right] = \sigma^2\mathbf{I}$ where σ is a constant. This result can be proved as follows. For the fixed value $|\epsilon_1|$, changing ϵ_1 from positive to negative is equivalent to reordering the vector $\mathbf{X}$ from $[s_1[1]\ s_2[1]\ s_1[2]\ s_2[2]\ \cdots\ s_1[N]\ s_2[N]]^T$ to $[s_2[N]\ s_1[N]\ s_2[N-1]\ s_1[N-1]\ \cdots\ s_2[1]\ s_1[1]]^T$. Since $\mathbb{E}\left[\mathbf{X}\mathbf{X}^H\right] = \mathbf{I}$ and $\mathbb{E}\left[\mathbf{H}\mathbf{H}^H\right] = \sigma^2\mathbf{I}$, the order of entries in $\mathbf{X}$ has no effect on the average throughput. As a result, the rate loss function Δ_{ϵ_1} is symmetric with respect to $\epsilon_1 = 0$.

B. Impact of Coordination Timing Error

We now investigate the impact of the coordination timing error on the throughput loss and still consider the practical scenario where the error is relatively small, such that $\epsilon_1 = 0$ and $\epsilon_2 \ll 1$.

By omitting high-order terms of ϵ_2, we obtain the throughput loss incurred by the coordination timing error from (21) as

$$\begin{aligned}\Delta_{\epsilon_2} = &-\frac{1}{N}\mathbb{E}\Big\{\log\det\Big[\mathbf{I}_{2N}+\epsilon_2\left(\mathbf{I}_{2N}+\mathbf{H}\mathbf{H}^H\mathbf{R}\right)^{-1}\Big(\mathbf{H}\mathbf{H}^H\mathbf{Z}_2^H \\ &+(\mathbf{R}+\epsilon_2\mathbf{Z}_3)^{-1}(\mathbf{Z}_2-\mathbf{Z}_3)\mathbf{H}\mathbf{H}^H(\mathbf{R}+\epsilon_2\mathbf{Z}_2^H)\Big)\Big]\Big\} \\ &\overset{(a)}{\approx} \epsilon_2 c_2, \end{aligned} \tag{23}$$

where $\mathbf{F}_2 = \left(\mathbf{I}_{2N}+\mathbf{H}\mathbf{H}^H\mathbf{R}\right)^{-1}\left(\mathbf{H}\mathbf{H}^H\mathbf{Z}_2^H+\mathbf{R}^{-1}(\mathbf{Z}_2-\mathbf{Z}_3)\mathbf{H}\mathbf{H}^H\mathbf{R}\right)$, $c_2 = -\frac{1}{N}\mathbb{E}\left[\mathrm{Tr}(\mathbf{F}_2)\right]$, and (a) can be derived by following the same steps in the derivation of (22). From (23), we note that the rate loss is approximately linear to ϵ_2 when $\epsilon_1 = 0$ and $\epsilon_2 \ll 1$.

V. Numerical Results

In this section, we present numerical results to illustrate the impact of timing error on the performance of ANOMA systems. In our simulations, we set the symbol length $T = 1$ and the transmitted signal power $P_1 = P_2 = 1$. If not specified, the intended timing mismatch between the two signals is set to $\tau = 0.5$, which is the optimal timing mismatch for ANOMA systems to achieve the best throughput performance [10]. We adopt the Rayleigh fading channel model with $\mathbb{E}[|h_1|^2] = 1$ and $\mathbb{E}[|h_2|^2] = 0.5$. In addition, the throughput loss ratio is defined as

$$\gamma = \frac{\Delta}{R}. \tag{24}$$

We first evaluate the impact of timing errors on the throughput of ANOMA systems. Fig. 4 presents the rate loss ratio as a function of ϵ_1 and ϵ_2 ranging from -0.1 to 0.1. As shown in Fig. 4, Δ is a continuous function with respect to ϵ_1 and ϵ_2 but non-differentiable when $\epsilon_1 = 0$ or $\epsilon_1 + \epsilon_2 = 0$. This is because there are non-linear step functions in the expression of $\mathbf{E}_1$ in (14).

We also study the individual effects of the timing synchronization error and the coordination timing error on the throughput of ANOMA systems. In Fig. 5, we show the throughput loss ratio as a function of ϵ_1 when $\epsilon_2 = 0$ and ϵ_2 when $\epsilon_1 = 0$. Note that the curves with the legends "impact of ϵ_1" and "impact of ϵ_2" are the slices of Fig. 4 when $\epsilon_2 = 0$ and $\epsilon_1 = 0$, respectively. The approximated results are calculated by Δ_{ϵ_1}/R and Δ_{ϵ_2}/R using (22) and (23). It is demonstrated that the expressions in (22) and (23) are good approximations of (21) when $|\epsilon_1| < 0.05$ and $|\epsilon_2| < 0.05$, respectively. Besides, ϵ_1 causes almost twice rate loss than that incurred by ϵ_2 for the same value of error. This phenomenon reveals that the performance of ANOMA is more sensitive to the synchronization timing error ϵ_1 than the coordination timing error ϵ_2. This also explains why the oversampling technique with a system with timing mismatch can still outperform a synchronized system when the timing mismatch information is unknown [14].

We further study the individual impacts of the timing synchronization error and the coordination timing error on the throughput of ANOMA when the errors are large. In Fig. 6, we present the throughput loss ratio as the function of the timing error where the value of ϵ_1 is chosen from $[\tau - T, \tau]$ (which is [-0.5, 0.5]) when $\epsilon_2 = 0$ and the value of ϵ_2 is chosen from $[-\tau, T - \tau]$ (which is [-0.5, 0.5]) when $\epsilon_1 = 0$. If $\epsilon_1 = 0$, it is shown that the rate loss ratio increases with the absolute

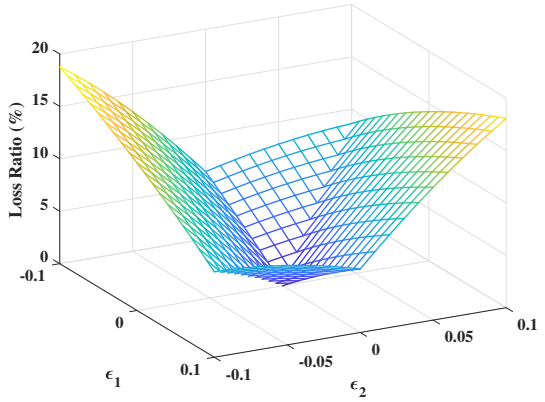

Fig. 4: The rate loss ratio as a function of ϵ_1 and ϵ_2 when $\tau = 0.5$ and $N = 10$.

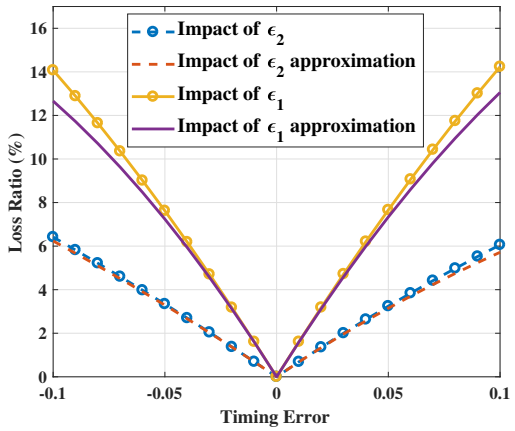

Fig. 5: The individual impacts of ϵ_1 and ϵ_2 on the rate loss ratio.

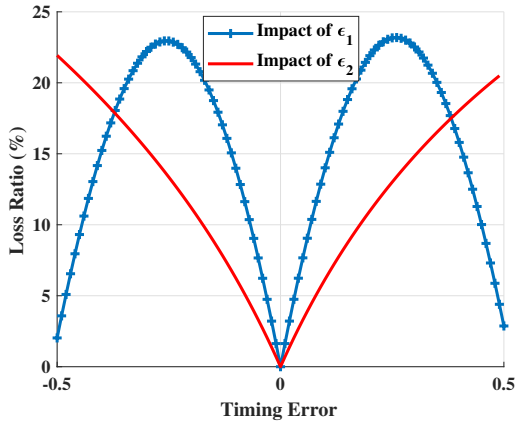

Fig. 6: The individual impacts of ϵ_1 and ϵ_2 on the rate loss ratio for the timing error ranging from -0.5 to 0.5.

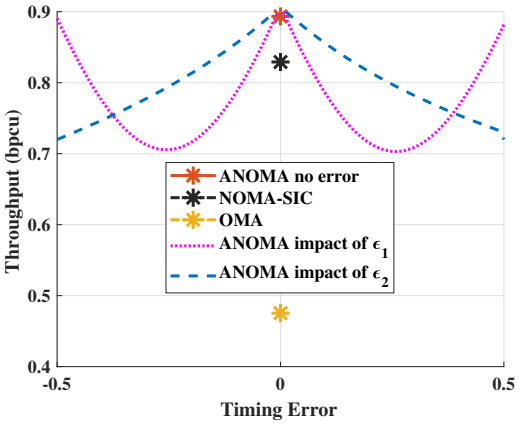

Fig. 7: Comparison of throughputs among OMA, NOMA, and ANOMA.

value of ϵ_2 monotonously. In contrast, as the absolute value of ϵ_1 increases, the rate loss ratio increases at the beginning and then decreases. This phenomenon can be explained as follows: if there is no timing error ($\epsilon_1 = \epsilon_2 = 0$), the sampling moments are at iT and $(i+0.5)T$, $i = 1, \cdots, N$. If $|\epsilon_1| = 0.5$ and $\epsilon_2 = 0$, the sampling moments are at $(i \pm 0.5)T$ and $(i+1\pm0.5)T$, $i = 1, \cdots, N$, which are equivalent to advancing ($\epsilon_1 = -0.5$) or delaying ($\epsilon_1 = 0.5$) all sampling moments by $0.5T$. The sampling diversity can still be achieved except that there will be rate loss due to the shift of sampling moments. For the case $\epsilon_1 = 0$ and $|\epsilon_2| = 0.5$, the second sample vector is a duplicate ($\epsilon_2 = -0.5$) or a shifted version ($\epsilon_2 = 0.5$) of the first sample vector. Hence, the sampling diversity cannot be obtained and only the first sample vector can be used to recover the transmit symbols.

Finally, we compare the performances of OMA, NOMA, ANOMA, and ANOMA with the timing error in Fig. 7. In our simulation, the conventional TDMA is adopted as the OMA scheme. As shown in the figure, the throughput curves of OMA, synchronous NOMA, and ANOMA with no error are single points because they are not functions of ϵ_1 or ϵ_2. It is demonstrated that the rate performance for ANOMA with no error is better than that of NOMA with SIC which is further greater than that of OMA. This aligns with the conclusion in [10]. We note that the ANOMA with timing error does not always outperform a perfectly synchronized NOMA. However, for small timing errors, ANOMA outperforms even a perfectly synchronized NOMA. On the other hand, ANOMA always outperforms a perfectly synchronized OMA.

VI. Conclusion

In this paper, we have studied the impact of two types of timing errors on ANOMA systems, i.e., the synchronization timing error and the coordination timing error. We have shown how these two errors jointly and separately affect the throughput performance of ANOMA systems. We have found that the ANOMA system is more sensitive to the synchronization timing error than the coordination timing error. From the design perspective of the ANOMA, our finding indicates that eliminating the synchronization timing error is more important than reducing the coordination timing error.

References

[1] R. Razavi, M. Dianati, and M. A. Imran, "Non-orthogonal multiple access (NOMA) for future radio access," in *5G Mobile Communications*. Springer, Oct. 2017, pp. 135–163.

[2] X. Liu and H. Jafarkhani, "Downlink non-orthogonal multiple access with limited feedback," *IEEE Trans. Wireless Commun.*, vol. 16, pp. 6151–6164, Sep. 2017.

[3] S. Verdu, "The capacity region of the symbol-asynchronous Gaussian multiple-access channel," *IEEE Trans. Inf. Theory*, vol. 35, no. 4, pp. 733–751, Jul. 1989.

[4] X. Zou and H. Jafarkhani, "Asynchronous channel training in massive MIMO systems," in *Proc. IEEE Global Communications Conference (GLOBECOM)*, Washington, DC, USA, Dec. 2016, pp. 1–6.

[5] A. Das and B. D. Rao, "MIMO systems with intentional timing offset," *EURASIP Journal on Advances in Signal Processing*, vol. 2011, no. 1, pp. 1–14, Dec. 2011.

[6] K. Barman and O. Dabeer, "Capacity of MIMO systems with asynchronous PAM," *IEEE Trans. Commun.*, vol. 57, no. 11, pp. 3366–3375, Nov. 2009.

[7] S. Poorkasmaei and H. Jafarkhani, "Asynchronous orthogonal differential decoding for multiple access channels," *IEEE Trans. Wireless Commun.*, vol. 14, no. 1, pp. 481–493, Jan. 2015.

[8] M. Ganji and H. Jafarkhani, "Interference mitigation using asynchronous transmission and sampling diversity," in *Proc. IEEE Global Communications Conference (GLOBECOM)*, Washington, DC, USA, Dec. 2016, pp. 1–6.

[9] X. Zhang, M. Ganji, and H. Jafarkhani, "Exploiting asynchronous signaling for multiuser cooperative networks with analog network coding," in *Proc. IEEE Wireless Communications and Networking Conference (WCNC)*, San Francisco, CA, USA, Mar. 2017, pp. 1–6.

[10] J. Cui, G. Dong, S. Zhang, H. Li, and G. Feng, "Asynchronous NOMA for downlink transmissions," *IEEE Commun. Lett.*, vol. 21, no. 2, pp. 402–405, Oct. 2017.

[11] *Release 10: Physical Layer Procedures for Evolved Universal Terrestrial Radio Access (E-UTRA)*. document TS 36.213, v10.1.0, Apr. 2011.

[12] Y. Mostofi and D. C. Cox, "Mathematical analysis of the impact of timing synchronization errors on the performance of an OFDM system," *IEEE Trans. Commun.*, vol. 54, no. 2, pp. 226–230, Feb. 2006.

[13] J. R. Magnus and H. Neudecker, *Matrix differential calculus with applications in statistics and econometrics*. NYC, NY: Wiley series in probability and mathematical statistics, 1988.

[14] M. Avendi and H. Jafarkhani, "Differential distributed space-time coding with imperfect synchronization in frequency-selective channels," *IEEE Trans. Wireless Commun.*, vol. 14, no. 4, pp. 1811–1822, Apr. 2015.